Nanotechnology Perceptions
ISSN 1660-6795
www.nano-ntp.com

Adaptive Sea-Clutter Model Based Detection for Coastal Surveillance Radar

R. Navya[1], Devaraju Ramakrishna[2], Sneha Sharma[3]

[1]Assistant Professor & Research Scholar, Department of Electronics and Communication Engineering, Dayananda Sagar University, Bengaluru, India, navya-ece@dsu.edu.in
[2]Associate Professor, Department of Electronics and Telecommunication Engineering, Dayananda Sagar College of Engineering, Bengaluru, India, devaraju-tce@dayanandasagar.edu
3Assistant Professor, Department of Electronics and Communication Engineering, Dayananda Sagar University, Bengaluru, India, sneha-ece@gmail.com

In order to analyse marine clutter amplitude statics and dynamically fit the optimal standard model for a particular data set extracted from a surveillance region, this research article aims to design a software module. There exists many theoretical and experimental work on understanding sea clutter behaviour & different statistical models used for representing amplitude distributions, such as Log-normal distribution, Weibull Distribution and K-Distribution. This research paper intends to study the statistical characteristics of unprocessed amplitude returns from E-band coastal surveillance radar after application of Sensitivity Time Control and Analogue-to-Digital conversion. The histogram of unique data samples (de-correlated in space) in a chosen analysis area is computed. This data is used to obtain a fit with standard distributions mentioned above. The shape & scale parameters of standard distributions are estimated & Probability density function of those distributions are computed. Root Mean square error value is computed for each estimated model data with respect to the histogram of original dataset. The model with least Root Mean Square Error value is the best fit for given sampled data. The estimated parameters for the best statistical fit for sea clutter in a particular sector is then passed on to detection module in order to determine the sea-clutter model based detection threshold level.

Keywords: Sea Clutter Amplitude Statistics, Log-normal distribution, Weibull Distribution, K-Distribution formatting, Sensitivity Time Control (STC), Analogue-to-Digital Conversion, Probability Density Function (PDF), Root Mean Square Error(RMSE), Range & Azimuth.

1. Introduction

Marine echoes, often referred to as sea clutter, are radar signals that are backscattered from the sea surface and are an inevitable occurrence for radars operating in maritime situations. Radar's main objective for some applications, such remote sensing systems, can be to capture

this backscatter signal. Sea backscatter is unwanted for other applications and can cause radar performance issues.

The characteristics of Sea clutter can vary significantly depending on geographic location, season, and current environmental conditions. While designing the Radar systems these characteristics need to be considered to design appropriate signal processing methods for performance evaluation in varying situation.

To achieve this, important step would be to design statistical model for the data of clutter returns with more accuracy. Developed models should be able to consider critical characteristics of the clutter returns like spatial and temporal behavior.

Generally, clutter echo is modelled using the variety of properties, such as surface reflectance σ0, intensity distribution of clutter. Discrete clutter spikes, the polarisation scattering matrix, the clutter return spectrum, and the clutter return spatial variation. Area reflectivity determines the average Radar Cross-Section (RCS) (Parthiban et al., 2004; Hui et al., 2015) of the clutter echo per unit.

The statistical behavior of the clutter echo from multiple thickly distributed scatters is generally used to characterize sea clutter; however, discrete scatters or isolated clutter spikes can also be observed and characterized, and then included into standard distributed clutter models.

In Radar, grazing angle (M, A, Jabeen et al., 2014) is defined as the angle formed between the line drawn from the Radar sensor to a target on the surface and a tangent to the earth at the desired target's location. Typically grazing angle is less than 100 at the surface of the sea. and the area of consideration frequently stretches to the radar horizon. Echo from the sea can frequently resemble targets in these circumstances and can be quite challenging to differentiate from actual targets. The region where wind causes ocean waves to form. also describes the fetch area's length, measured with the wind in its direction.

How the shape of the maritime clutter reflectance changes with grazing angle as seen in microwave Backscatter from the sea surface is due to the multiple reflection caused due to rough sea surface. Statistical models for backscattering uses a variety of irregular surface descriptions and approximations method to consider the scattering pattern.

It is possible to simulate scattering from nearby wind-derived waves using Bragg (or resonant) scattering (Schoenecker et al.,2016). Longer waves on the sea cause ripples to tilt, which modifies the intensity of the scattered signals. This tilt effect is considered while creating composite model.

Clutter reflectivity is commonly expressed as the normalised sea clutter Radar cross section, divided by illuminated surface area, σ^0.

Figure 1, depicts how the shape of the maritime clutter reflectance changes with grazing angle as seen in microwave radar. Backscatter for a typical I-band radar with respect to wind speed around 15 KN is demonstrated in below example (Watts,2013).

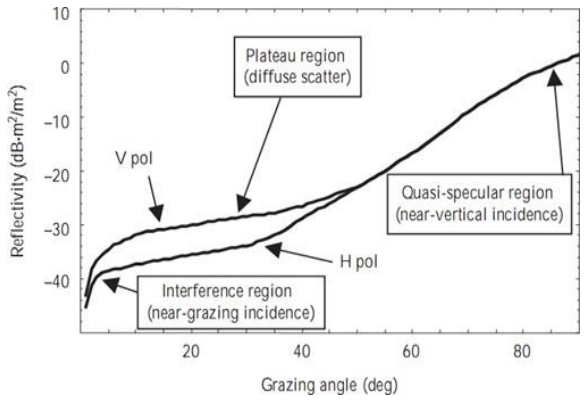

Figure 1. Sea clutter reflectivity v/s grazing angle

The incidence in quasi-specular backscattering is almost vertical (Watts, 2008; Rosenberg et al.,2019). When viewed from a completely flat surface, in quasi-specular region backscatter varies inversely with roughness of the sea surface, peaking at perpendicular incidence. At medium grazing angles, the reflectance shows less dependence on grazing angle, as this sample below around 50˚ from grazing illustrates; this region is sometimes called the plateau region. It is found that in interference region, which is often approximately 100 from grazing (critical angle) depending on roughness of sea surface, the sea reflectivity declines much quicker with decreasing grazing angles.

2. Amplitude Statistics of Sea Clutter:

The E-band radar, which solely uses the received signal's envelope for signal processing, is the one being examined in this investigation. Non-coherent statistics can be characterised using the envelope of the return which follows a square law detector of the radar return power.

The mean clutter power is represented by the area reflectivity σ0. A single radar resolution cell's instantaneous power output ranges around this mean value. The PDF of the returns describes this variation.

The fluctuations are mostly caused by two factors:

- Firstly, depending on the grazing angle, rough surface, sea state, density of ripple, and supplementary multiple factors responsible with the flow of long waves. Backscatter caused due to small local areas fluctuates significantly around the mean of reflectivity.

- Secondly, numerous tiny structures (commonly referred to as scatters) inside a radar resolution patch scatter, moving in relation to one another and interfering with the scattered signal (sometimes called speckle).

Speckle is frequently explained as the product of a Gaussian scattering (Xue et.al.,2019) statistics-exhibiting uniform field of several random scatters. The PDF of these clutter returns amplitude, E, is represented by the Rayleigh distribution:

$$P(E) = \frac{2E}{x}\exp\left(\frac{-E^2}{x}\right) ; 0 \leq E \leq \square \qquad (1)$$

where the average value of E, ⟨E⟩ = ($\sqrt{\pi}$_x)/2; the mean square ⟨En⟩ = x; and the higher moments

$\langle En \rangle = x^{n}/_{2}\ \gamma(1 + \frac{n}{2})$;

By using a square-law detector, intensity of returns (Watts, 2008) PDF can be obtained as follows:

$P(z) = \frac{1}{x} \exp^{(\frac{-z}{x})}$; $0 \leq z \leq$ □ (2)

here $z = E^2$, (z) = x & $\langle z^n \rangle = n!\ x^n$

When grazing angles exceed around 10˚ and dimensions of range cell is much bigger compared to wavelength sea swell, clutter is commonly defined as speckle with a Rayleigh distributed amplitude on radars with low spatial resolution.

When a radar employs frequency agility, clutter echo often has very small temporal decorrelation durations between 5 and 10ms and are rather heavily decorrelated from pulse to pulse. With increased radar resolution and at lesser grazing angles, the clutter amplitude distribution is observed to have an extended tail and the clutter returns are sometimes described as becoming spiky.

The high-resolution clutter amplitude has aspects of temporal and spatial correlation that are different from the speckle distribution and exhibit deviations from the Rayleigh distribution. Specifically, clutter no longer decorrelates with frequency agility, and correlation durations that were formerly milliseconds now reach seconds.

2.1 Sea Clutter Amplitude Statistics Nature

Measurements of low grazing angle, high-resolution sea clutter returns have revealed two critical parameters of the intensity fluctuations.

First, a spatially fluctuating mean level is produced by set scattering of data points of with the long sea surface waves and wave complexity of the ocean. This property is independent of frequency agility and has a lengthy correlation time, because the clutter return in any resolution cell has numerous scatters, there is also a second speckle component. This can be related by using frequency agility or the scatters relative motion.

2.2 Coherent Features of Sea Clutter in Radar

Targets with a high enough radial velocity (Raynal, 2010) can be distinguished from clutter by coherent radars using Doppler processing. Nevertheless, the Doppler shifts of certain interesting targets won't differ all that much from the clutter's Doppler spectrum. Under such circumstances, for each potential situation, the designer of radars must have a complete knowledge of properties the Doppler spectrum.

3. Low Grazing Angle Statistics

Many models of the distribution of marine clutter amplitude have been created in an effort to functionally represent the observed distributions. The following are the three most popular

models namely Lognormal distribution, Weibull distribution, K distribution.

3.1. The Log-Normal Distribution

For the lognormal (Crisp et al.,2009; Ding et.al.,2020) the probability density function (PDF) of intensity z is as follows:

$$P(z) = \frac{1}{\sqrt[z]{2\Pi\sigma^2}} \boldsymbol{exp}\left(-\frac{(log_e^{[z]}-\mu)^2}{2}\right); \boldsymbol{z > 0} \qquad (3)$$

μ → scale parameter , σ → shape parameter.

The distribution's mean (μ) and variance (σ2) are taken from a Gaussian (Yunhan Dong,2004) or normal distribution, of loge[z]. When low grazing angles are detected by a high resolution, horizontal polarisation radar, the statistics of sea clutter are similar to those of the log-normal distribution. ($\phi < 5^{\circ}$).

In general, the dynamic range of the real clutter distribution is typically overestimated by the Log-Normal model and underestimated by the Rayleigh model.

From the perspective of detection, the Rayleigh distribution represents the best situation, whereas the Log-Normal distribution represents the worst-case scenario.

3.2. Estimation of Parameters for Log-Normal Distribution

The Maximum Likelihood (ML) estimate is a commonly used method for parameter estimation since it yields the best parameter estimates without requiring any prior knowledge about the data.

The joint PDF is the product of the marginal PDFs if 'n' independent samples Z1, Z2..., Zn are taken from a distribution with 'm' parameters θ1, θ2, θ3… θm.

The most likely collection of parameter values given the observed data is the ML estimate, which maximises the likelihood function's value. The ML estimate will maximise the log-likelihood function as well because the logarithm function is a monotonic function.

$$\sum_{i=1}^{n} \boldsymbol{Ln}(\mu, \boldsymbol{\sigma^2}; \boldsymbol{z_i}) \qquad (4)$$

ML estimations of the parameter are obtained by taking the derivative of equation (4) with respect to the parameters μ & σ2, and setting each to zero.

$$\widehat{\boldsymbol{\mu}}_{\boldsymbol{ML}} = \frac{1}{n}\sum_{i=1}^{n} \boldsymbol{ln}(\boldsymbol{z_i}) \qquad (5)$$

$$\widehat{\boldsymbol{\sigma}}_{\boldsymbol{ML}} = \sum_{i=1}^{n} [\boldsymbol{ln}\,(\boldsymbol{z_i}) - \widehat{\boldsymbol{\mu}}_{\boldsymbol{ML}}]^2 \qquad (6)$$

An accurate estimate of σ2 is provided by equation (6), albeit it is biased. This defines an impartial appraisal of a2:

$$(\widehat{\boldsymbol{\sigma}}_{\boldsymbol{ML}})_{\boldsymbol{unb}} = \frac{1}{(n-1)} \sum_{i=1}^{n} [\boldsymbol{ln}\,(\boldsymbol{z_i}) - \widehat{\boldsymbol{\mu}}_{\boldsymbol{ML}}]^2 \qquad (7)$$

3.3. The Weibull Distribution

The Weibull PDF (Xueli et.al.,2019) is a distribution with two parameters, of which the Rayleigh distribution is a particular instance. The skewness of the distribution is related to the first parameter of the distribution, the shape parameter, while the distribution is scaled by the second value, the scale parameter.

When there is low grazing angle or high resolution, the Weibull PDF is recognised to depict marine debris fairly well. When shape and scale parameters are estimated correctly, the necessary spikiness and power characteristics of the returning echo signal can be simulated.

The Weibull model has a PDF (Watts, 2008):

$$P(z) = \frac{\gamma}{\bar{\omega}}\left(\frac{z}{\bar{\omega}}\right)^{\gamma-1} \boldsymbol{exp}\,(-(\frac{z}{\bar{\omega}})\,\gamma)\;;\; z \geq 0;\; \gamma \geq 0;\; \bar{\omega} \geq \mathbf{0} \quad (8)$$

where the scale parameter is denoted by $\bar{\omega}$ and the shape parameter by γ.

3.4. Estimation of Parameters for Weibull Distribution

The ML estimates do not provide closed form solution. An iterative estimation method proposed by Menon provides estimates resulting in the selection of a false alarm rate for every value of γ and ω. The estimators are:

$$\hat{\gamma}_{Men}=\{\left\{\frac{6}{\pi^2}\frac{n}{n-1}\right.[\frac{1}{n}\sum_{i=1}^{n}(\boldsymbol{ln}(z_i)^2-(\frac{1}{n}\sum_{i=1}^{n}\boldsymbol{ln}\,(z_i))^2]\}^2 \quad (9)$$

$$\hat{\omega}=\exp[\frac{1}{n}\sum_{i=1}^{n}\boldsymbol{ln}(z_i)+\mathbf{0.5772}\,\hat{\gamma}_{Men}{}^{-1}] \quad (10)$$

3.5. The K-Distribution

Sea clutter can be limited by the K-distribution, as demonstrated by the statistical outcomes of numerous tests conducted in the last few years. Under the radar beam, the received signal is interpreted by the K-distribution as a superposition of returns from several independent scatters.

Two prominent components that have distinct correlation times and contribute to the amplitude distribution are revealed by analysis of the sea clutter data.

Due to a scattered bunching connected to the long sea waves and swell structure, the spatially variable mean level is the first component. This is a frequency agility-insensitive component with a lengthy correlation time. The second "speckle" component arises from the clutter's numerous distributed characteristic in any range cell.

This can be related by using frequency agility or the scatters relative motion.

The speckle component of the compound K distribution has an exponential PDF of amplitude z with average x (Parthiban & Madhavan. et.al., 2004).

$$P(z|x) = \frac{1}{x}\,\boldsymbol{exp}^{-\frac{z}{x}} \quad (11)$$

where a gamma PDF modulates x.

$$P_c(x) = \frac{b^v}{\Gamma(v)} x^{v-1} exp^{-bx} \quad (12)$$

Using the parameters v for shape and b for scale (Watts & Rosenberg, 2013).

In contrast to other models, comparison reveals that:

- When the shape parameter of the k-distribution equals infinity, it reduces to the Rayleigh distribution.
- Compared to the k-distribution, the Log-Normal distribution is consistently spikier.
- The k-distribution and the Weibull are equal when the shape parameter is set to 0.5. Both distributions are quite similar throughout a wide range of shape parameter values; for higher values, the k-distribution is somewhat spikier than the Weibull, and for lower values, it is slightly less spiky.

3.6. Estimation of Parameters for K-Distribution

In real clutter, estimating local statistics directly and setting a threshold appropriately is the best method for adaptive detection. It is obvious that the accuracy achievable will rely on the size of the clutter patch used to estimate the statistics and the response rate needed in settings that change over time, like the transition from land to shallow waters in the sea.

The total amplitude of the sea clutter returns in the K-distribution model (Baker, 1986) is given by two independent random variables as below:

$$a = y.v \quad (13)$$

where K_{v-1} (ca) is vth order modified Bessel function of second kind, and c = $\sqrt{\pi d}$ is scale parameter.

- The K-distribution decreases to the Rayleigh distribution when its shape parameter reaches infinity.
- Compared to the K-distribution, the Log-Normal distribution normally shows more spikes.
- Weibull distribution and the k-distribution are the same when the shape parameter is set to 0.5.

3.7. RMS Error Calculation to find best fit

A regression models that fits well yields projected values in radar applications that are in close agreement with the observed data values, particularly in the low Pfa region (i.e., Pfa < 0.1).

Clutter statistics (Crisp & Rosenberg. et.al., 2009; Zhao et.al., 2023) can be evaluated for model fit using the Root Mean Square Error (RMSE).

$$\text{MSE} = \frac{\sum_{i=1}^{K} \left(P_i^z - P_i^{est}\right)^2}{k} \quad (16)$$

where P_i^z denotes the measured frequency of a clutter sample with an amplitude falling between $i^{th}$and For the statistical model, $P_i^{est}$is the estimated number of occurrences in the

i^{th} interval. The low Pfa region of the statistical model is divided into K intervals.

In practice, as the histogram offset is removed we can achieve Pfa < 0.1 by calculating RMSE between observed occurrences and estimated occurrences, by leaving first 10 -15 intervals for the calculation.

The statistical model giving least RMSE is the best fit for given dataset.

4. Proposed Sea Clutter Model Based Detection

A non-Rayleigh distribution is found to govern the weather clutter seen by an S-band radar. To reduce this kind of noise and identify targets, a new CFAR circuit must be designed. Our advantage will be economic in nature if we can implement the new CFAR circuit by changing the LOG/CFAR circuit that has already been applied in real-world scenarios. Results show that for many tiny data including goals, the log-normal distribution fits the data the best.

4.1. Log-Normal Threshold Calculation:

For lognormal distributions (Baker,1996), the probability density function (PDF) of the intensity z provided is known to exist by:

$$\boldsymbol{P_{LN}(z)} = \frac{1}{z\sqrt{2\pi\sigma^2}}\boldsymbol{exp}\left(-\frac{\boldsymbol{log_e^{[z]-\mu^2}}}{2\sigma^2}\right); \text{ z > 0 … from equation (3)}$$

where μ & u are the scale and shape parameters, respectively.

Assuming that a comparator converts the signal z < Th to z = 0 when a threshold level Th is applied to the signal z that follows the distribution provided by Equation (3), the false alarm probability PN is as follows:

$$\boldsymbol{P_N} = \int_{T_h}^{\infty}\boldsymbol{P_{LN}(z)dz} = \frac{1}{2}-\frac{1}{2}\boldsymbol{erf}\left(\frac{\boldsymbol{ln(T_h)}}{\sqrt{2}\sigma}\right) \qquad (17)$$

From equation (17), we can obtain an expression for calculating Th by fixing the value of PN & obtaining maximum likelihood estimate of shape parameter. A list of values of threshold obtained for various values of false-alarm probability and shape parameter estimate is shown below.

Table 1: Calculation of Threshold for various values of PN (Probability of false alarm) using Log-Normal shape parameter estimate $\boldsymbol{u_{est}}$.

P_N	T_h (expression)	u_{est}	T_h (value)	T_h
10^{-4}	exp(3.719* a_{est})	1.15	72.0132 + (fixed offset)	181
10^{-3}	exp (3.09 * a_{est})	1.15	34.9354 + (fixed offset)	144
10^{-2}	exp(2.3263*a_{esT})	1.15	14.516 + (fixed offset)	124

4.2. Weibull Threshold Calculation:

The Weibull model has a PDF:

$\boldsymbol{P_{wb}(z)} = \frac{\gamma}{\bar{\omega}}\left(\frac{z}{\bar{\omega}}\right)^{\gamma-1} \boldsymbol{exp}\left((\frac{z}{\bar{\omega}})^{\gamma}\right)$; z ≥ 0; $\boldsymbol{\gamma} \geq 0$; $\bar{\boldsymbol{\omega}} \geq 0$ from equation (8)

where the scale parameter is $\bar{\boldsymbol{\omega}}$ and the shape parameter is γ.

For Weibull clutter (Raynal,2010), the correlation between the threshold to mean and false-alarm probability can be computed using

$$\boldsymbol{P_N} = \int_{T_h}^{\infty} \boldsymbol{P_{wb}(z)dz} = \boldsymbol{exp}\left\{-\left(\frac{T_h}{\bar{\omega}}\right)^{\gamma}\right\} \qquad (18)$$

where b is the characteristic and γ is the form parameter value (63.2 percentile value) i.e. 0.632* $\bar{\boldsymbol{\omega}}$.

A typical experimental calculation is shown in table below:

Table 2: Calculation of Threshold for various values of PN (Probability of false alarm) using Weibull shape & scale parameter estimates yest & $\boldsymbol{w_{est}}$.

P_N	T_h (expression)	y_{est}	w_{est}	T_h (after adding offset (31))
10^{-4}	9.21^ (1/γ)*0.632*$\bar{\boldsymbol{\omega}}$	1.17	28.3	150
10^{-3}	9.21^ (1/γ)*0.632*$\bar{\boldsymbol{\omega}}$	1.17	28.3	124
10^{-2}	9.21^ (1/γ)*0.632*$\bar{\boldsymbol{\omega}}$	1.17	28.3	97

4.3. K-Distribution Threshold Calculation

We know that the overall amplitude of k-distributed clutter (D. J. Crisp, L. Rosenberg, 2009) is

$\boldsymbol{f_k(z)} = \frac{2c}{\Gamma(v)}\left(\frac{ca}{2}\right)^{v} \boldsymbol{\nu_{K_{v-1}}(ca)}$ from equation (12)

where c = $\sqrt{\pi}$d is the scaling parameter and $K_{v-1}(ca)$ is the v^{th} order modified Bessel function of second type.

The average level of clutter in this instance is

<E> = $\sqrt{\frac{\pi}{d}}\frac{\Gamma(\vartheta+0.5)}{2*\Gamma(\vartheta)}$

The relationship between false-alarm probability[3] and CFAT multiplier α_{FT} is:

$$P_{FA} = \frac{2}{\Gamma(v)}\ \alpha_{FT} \qquad (19)$$

From equation 19, we can compute Threshold for given PFA where α_{FT} = Threshold / mean clutter level.

4.4. System Interfacing Block Diagram

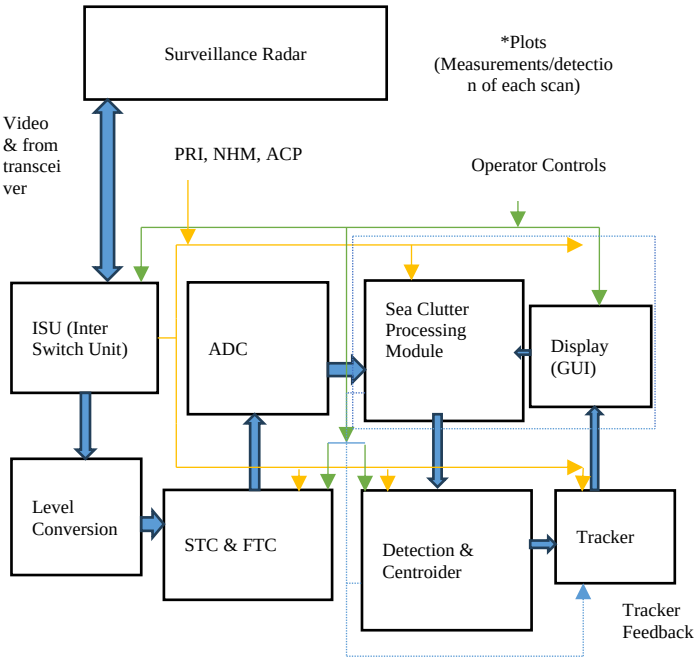

Figure 2. Signal flow diagram

4.5. Structure of Input Data to Clutter Analysis Module

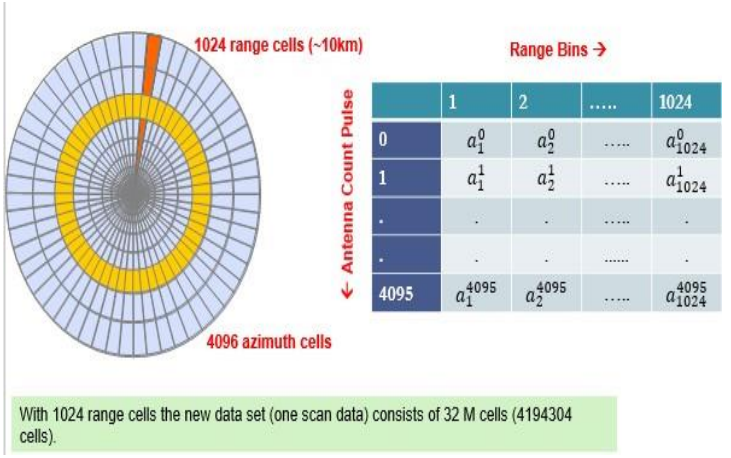

Figure 3. Representation of input dataset chosen for analysis

Figure (3), represents the structure of data received at the input of sea clutter processing module. The maximum unambiguous range for PRF = 1800Hz is around 80km. This range scale is divided into 8192(8K) range resolution cells. The azimuth angle is divided into 4096(4K) azimuth cells and an ACP signal is received at the beginning of each azimuth cell.

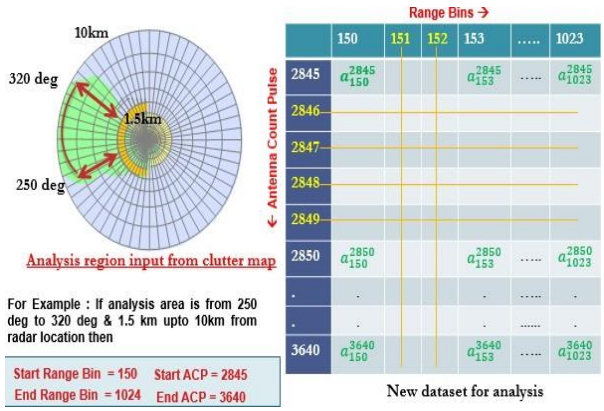

Figure 4. Decimation of values in dataset of analysis area for de-correlating sea clutter

Analysis for sea clutter is done for samples in first 10km range as strength of sea clutter returns is significant in first 5–10 km from coastline as shown in Figure (4).

Analysis dataset is decimated in both range bins and azimuth bins in order to de-correlate sea clutter and a histogram of resulting dataset is used for estimating parameters of standard sea clutter models as described in previous sections.

5. Results and Discussion

Matlab Analysis of one scan data obtained from s-band radar is plotted is as shown

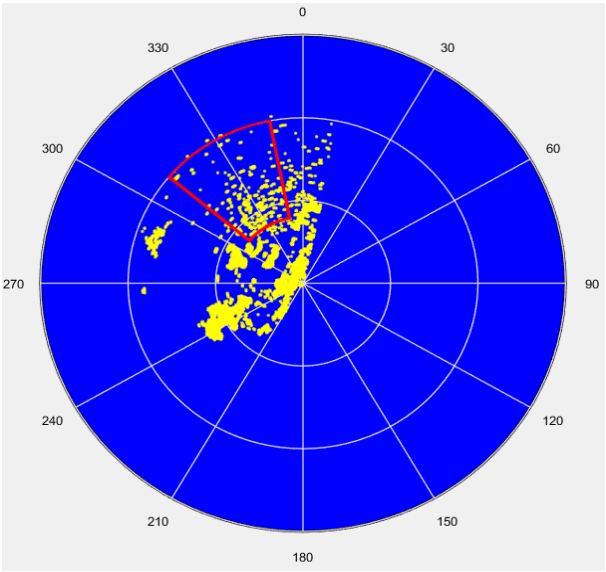

Figure 5. Polar chart of one scan data

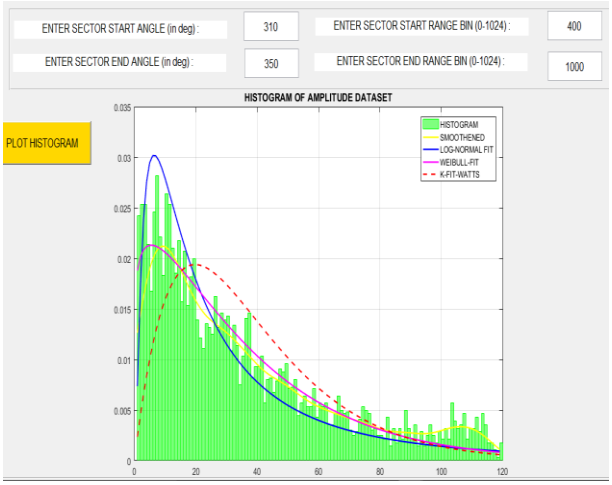

Figure 6. Histogram of one scan data with PDF of Log-Normal, Weibull, & K-Distribution Estimates

As shown in above Figure 5. Polar chart depicts the sea clutter return amplitude intensity at near range for the data set under consideration. Aa explained in previous sections histogram of the data set is generated as shown in Figure 6.

On the same set of data which is decimated in both range bins and azimuth bins RMSE is determined for each statistical model as shown in Figure 7. With this analysis result it is found that Log-Normal model is Best fit for the considered data set.

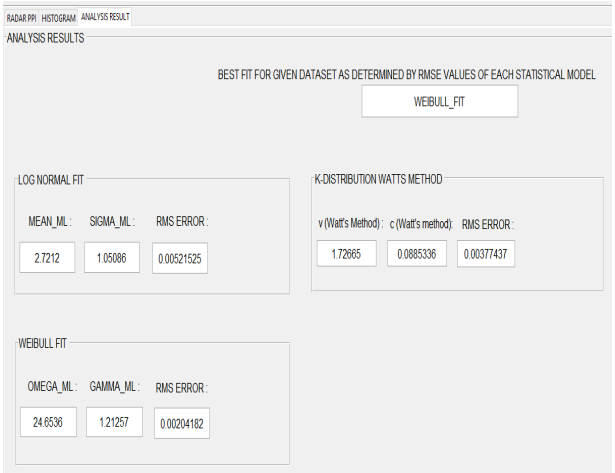

Figure 7. Root Mean Square Error Goodness of Fit Test Results for Selected Data of Analysis Area

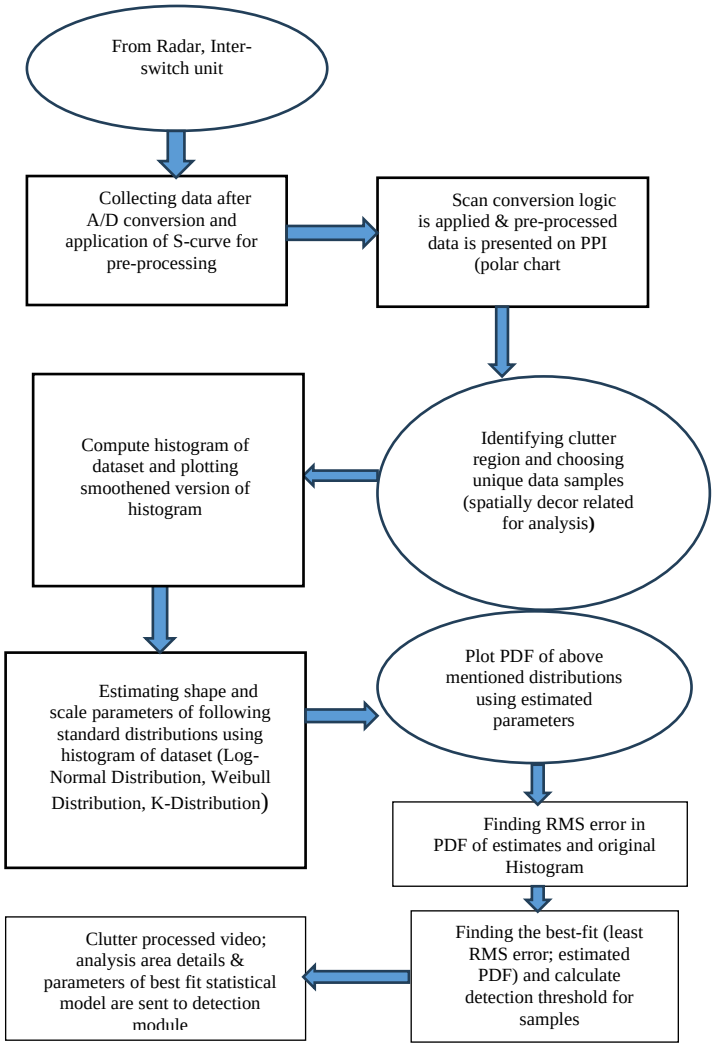

Figure 8. Flowchart of implementation

5.1 Implementation Results

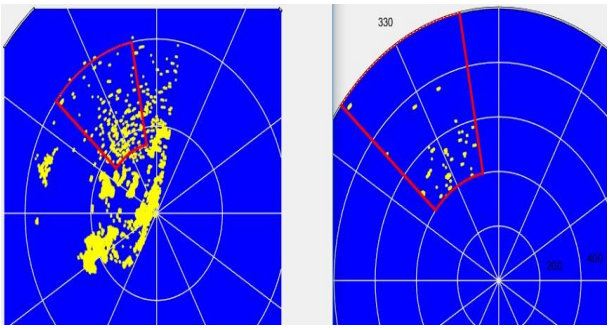

Figure 9. Polar chart before & after applying Log-Normal Threshold

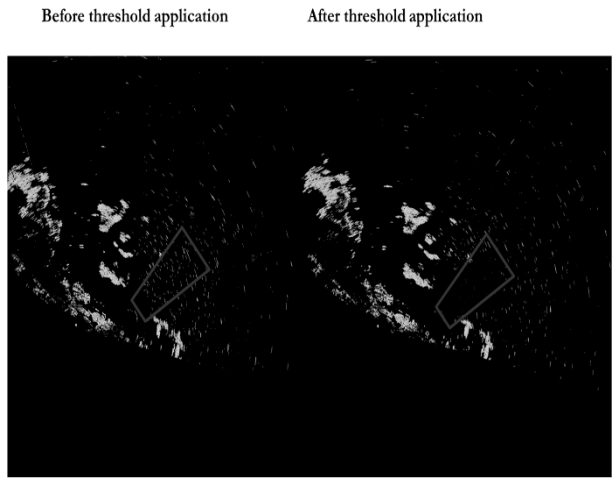

Figure 10. PPI showing analysis area without & with application of log-normal threshold

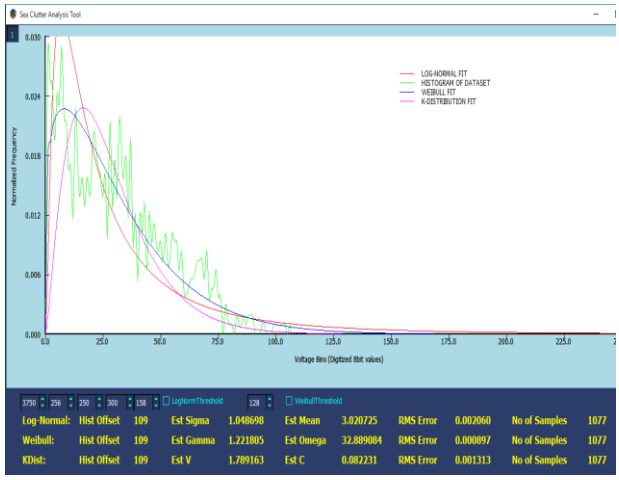

Figure 11. Histogram of recorded data with PDF & values of estimates

Once the calculated threshold is applied the input data set, clutter returns for the give region is reduced drastically as shown in Figure 9 and Figure 10. Figure 11 depicts the histogram of data set under consideration with PDF & values of estimates for each statistical model.

6. Conclusion

To validate the developed sea clutter models, a sufficient number of experimentally acquired data samples that meet the following criteria must be obtained:

- In order to eliminate the speckle component by averaging when determining the correlation length of the large-scale effects, each data set needs to contain several hundred returned pulses from each range bin.

- Several hundred returned pulses from each range bin are required in each data set to provide sufficient independent samples for analysis following subsampling, which eliminates data correlation.

- The ideal antenna beam shape must be chosen to minimise any impact on recorded data.

- To reduce the impact of noise on clutter characteristics, recorded data should have a high clutter-to-noise ratio.

Therefore, by validating these models for amplitude data collected during each scan, the system may adjust the detection threshold adaptively to suit the conditions of the sea.

References

1. Baker, C. J. (1986). Coherent Properties of K-Distributed Sea Clutter. 16th European Microwave Conference. https://doi.org/10.1109/euma.1986.334212
2. Bocquet, S. (2011). Calculation of radar probability of detection in K-Distributed sea clutter and noise. https://api.semanticscholar.org/CorpusID:131302889
3. Clutter Spatial Distribution and New Approaches of Parameter Estimation for Weibull and K-Distributions. (2004), Yunhan Dong DSTO-RR-0274.
4. Crisp, D. J., Rosenberg, L., Stacy, N. J., & Dong, Y. (2009). Modelling X-band sea clutter with the K-distribution: Shape parameter variation. IEEE International Radar Conference, 1–6. http://yadda.icm.edu.pl/yadda/element/bwmeta1.element.ieee-000005438411.
5. Ding, M., Li, Y., Quan, Y., Guo, L., & Xing, M. (2020). A Novel Reconstruction Method of K-Distributed Sea Clutter with Spatial–Temporal Correlation. Sensors, 20(8), 2377. https://doi.org/10.3390/s20082377
6. Hui, N. T., & Chonghua, N. F. (2015). Simulation of impact of sea clutter to radar detecting performance. International Symposium on Microwave, Antenna, Propagation, and EMC Technologies. https://doi.org/10.1109/mape.2015.7510330
7. M, A., Jabeen, F., Thakur, V., Department of ECE, KSSEM, Bangalore, India, & LRDE, DRDO, Bangalore, India. (2014). VHDL implementation of Scan-to-Scan discriminator for the detection of marine targets. International Journal of Engineering Research and Development, 10(11), 28–38. https://www.ijerd.com/paper/vol10-issue11/Version_1/E10112838.pdf
8. Parthiban, A., Madhavan, J., Radhakrishna, P., Savitha, D., & Kumar, L. (2005). Modeling and simulation of radar sea clutter using k-distribution. International Conference on Signal Processing and Communications, SPCOM. https://doi.org/10.1109/spcom.2004.1458425
9. Raynal, A. M., & Doerry, A. W. (2010). Doppler characteristics of sea clutter. https://doi.org/10.2172/992329
10. Rosenberg, L., Watts, S., & Greco, M. S. (2019). Modeling the statistics of microwave radar sea clutter. IEEE Aerospace and Electronic Systems Magazine, 34(10), 44–75. https://doi.org/10.1109/maes.2019.2901562
11. Schoenecker, S., Willett, P., & Bar-Shalom, Y. (2016). The effect of K-Distributed clutter on trackability. IEEE Transactions on Signal Processing, 64(2), 475–484. https://doi.org/10.1109/tsp.2015.2478745
12. Statistical Analysis of Northern Australian Coastline Sea Clutter Data. (2001) – Irina Antipov DSTO-TR-1236.
13. Watts, S. (2008). Radar sea clutter: Recent progress and future challenges. International

Conference on Radar. https://doi.org/10.1109/radar.2008.4653882
14. Watts, S., & Rosenberg, L. (2013). A review of high grazing angle sea-clutter. International Conference on Radar. https://doi.org/10.1109/radar.2013.6651992
15. Xue, J., Xu, S., Liu, J., & Shui, P. (2019). Model for Non-Gaussian sea clutter amplitudes using generalized inverse gaussian texture. IEEE Geoscience and Remote Sensing Letters, 16(6), 892–896. https://doi.org/10.1109/lgrs.2018.2886782
16. Xueli, P., Guisheng, L., Zhiwei, Y., & Hongxing, D. (2019). Experimental analysis of sea clutter using airborne circular scanning SAR in medium grazing angle. Chinese Journal of Systems Engineering and Electronics, 30(1), 68. https://doi.org/10.21629/jsee.2019.01.07
17. Zhao, X., Han, J., Zhang, X., Zhang, J., & Li, P. (2023). Sea clutter Measurement test and amplitude Characteristics analysis in the South China Sea nearshore area. Journal of Physics. Conference Series, 2486(1), 012022. https://doi.org/10.1088/1742-6596/2486/1/012022